A Three-layer Severity Index for Power System Voltage Stability Assessment using Time-series from Dynamic Simulations

Luigi Vanfretti, *Senior Member, IEEE* and Felix Rafael Segundo Sevilla, *Member, IEEE*

***Abstract*—This paper presents a three-layer voltage stability index computed using time-series obtained from dynamic simulations. The proposed index provides the distance with respect to voltage and power limits. Voltage, active and reactive power signals, which are determined using time series from dynamic simulations, are used to compute the index. The methodology assumes that no other information about the system (model) is available. A set of 3 different simulations at different loading levels and a given contingency are required to calculate the index. In the first layer, a two-element vector indicates if a power or a voltage limit was violated. In the second layer, a vector is used to specify which power and voltage loading level was violated and finally, in the third layer a matrix is used to retrieve precise information about which power and voltage limit has been violated in pre- or post- contingency. The index can analyze simultaneously different buses. The proposed index is illustrated using synthetic data and then tested using time-domain simulations on the KTH-Nordic32 system.**

***Index Terms*—voltage stability, single voltage source model, time-domain simulations, severity index**

I. Introduction

TODAY, methods to determine the likelihood of catastrophic system failures are necessary, as indicated by the negative impact of large-scale power outages in recent years [1]. The FP7 iTesla project aims to build a software toolbox to cope with these challenges. Dynamic impact assessment of detailed time-domain simulations is part of the off-line analysis workflow within the iTesla toolbox[1]. The aim is to develop offline criteria to support online analysis functions.

After performing a dynamic simulation for a specific contingency, an appropriate post-contingency severity index is determined in order to classify the impact of the contingency. To do so, a set of scalars, vectors and matrices namely severity indexes, provide a measure of how severe the contingency is. A three layer index has been designed with the requirement of fast computation because several contingencies have to be evaluated for each operating condition, and at the same time they must provide a good measure of how severe the contingency is. These requirements differentiate the voltage stability index presented here to those described in [2], [3] and [4].

This work was supported in part by the EU-funded FP7 iTesla project and by Statnett SF, the Norwegian Transmission System Operator.

L. Vanfretti and F. R. Segundo Sevilla are with the Electric Power Systems Department at KTH Royal Institute of Technology in Stockholm, Sweden (e-mail: *frss@kth.se* and *luigiv@kth.se*).

L. Vanfretti is with Statnett SF, Research & Development, Oslo, Norway (e-mail: *luigi.vanfretti@statnett.no*).

[1]iTESLA(Innovative Tools for Electrical System Security within Large Areas), online: www.itesla-project.eu

II. Equivalent Models of the Power System

Voltage Stability (VS) is a concern for power system security. Both static and dynamic analyses are used to investigate different aspects of voltage instability phenomena. However, when only time-series from dynamic simulations are available, it is necessary to identify a model from the time-series data. The approach proposed here is to identify a simple equivalent from the time-series of the simulations. The choice of the model used was made by considering the trade-off between model accuracy, speed to compute the stability limits, and the fact that no other information about the power system other than the time series was available.

Simple equivalent models of the power system and the load at a measurement point are estimated from the data, and then used for calculating power-voltage (PV) curves to predicting the stability limit [5].

A. Single Voltage Source Model

Let us consider the Thevenin equivalent of the power system as viewed from the measurement point. Figure 1 shows a single line diagram of the equivalent system. For simplicity, the network resistance is neglected. The equivalent model parameters $(E\angle\delta, X)$ are computed from time-series data (V_i, P_i, Q_i) as follows:

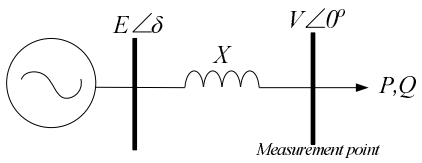

Fig. 1. Equivalent model

$$P = \frac{EV}{X}\sin\delta, \qquad Q = \frac{V(E\cos\delta - V)}{X} \tag{1}$$

Taking the last m samples at any instant of time yields:

$$\begin{aligned} P_i X - V_i E\sin\delta_i &= 0 \\ Q_i X - V_i E\cos\delta_i + V_i^2 &= 0 \end{aligned}, \quad i = 1,\cdots,m\cdot \tag{2}$$

With $2m$ equations in (2), only $m+2$ variables are unknown, i.e. the voltage E, the reactance X and the time-varying bus angles $\delta_i (i = 1,\cdots,m)$. Equation 2 is thus overdetermined,

and the model parameters are calculated solving the following least squares problem:

$$\underset{E,X,\delta_i}{min} \left\| \begin{array}{c} P_1X - V_1E\sin\delta_1 \\ Q_1X - V_1E\cos\delta_1 + V_1^2 \\ \vdots \\ P_mX - V_mE\sin\delta_m \\ Q_mX - V_mE\cos\delta_m + V_m^2 \end{array} \right\|. \quad (3)$$

B. Load Model

Equation $Q = \alpha + \beta P$ describes the linear P-Q load side model. Using the same data samples as in Section II-A, α and β are the solution of the following least square problem:

$$\underset{\alpha,\beta}{min} \left\| \begin{bmatrix} 1 & P_1 \\ & \vdots \\ 1 & P_m \end{bmatrix} \begin{bmatrix} \alpha \\ \beta \end{bmatrix} - \begin{bmatrix} Q_1 \\ \vdots \\ Q_m \end{bmatrix} \right\| \quad (4)$$

The single voltage source model of Figure 1 can be combined with the linear P-Q load side model to calculate the PV characteristic and the voltage stability limit for the power transfer at the study point by solving (5)

$$P^2X^2 - E^2V^2 + (\alpha X + \beta PX + V^2)^2 = 0. \quad (5)$$

III. Three-Layer Severity Index

The proposed VS index provides a measure of how far the system is from the maximum loadability limit. Observe that in order to obtain a valid model from the identification process in Section II-B, at least 3 sets of time-series with different loading levels are required: (a) low, (b) acceptable and (c) heavy (unacceptable for operational standards) levels.

Combining this data, two different PV curves can be estimated, as shown in Figure 2. The pairs (P_a, V_a), (P_b, V_b) and (P_c, V_c) correspond to the averages from the time-window chosen from the dynamic simulation outputs of power and voltage at low, acceptable and heavy loading levels, respectively, in pre-contingency, while the pairs $(\hat{P}_a, \hat{V}_a)$, $(\hat{P}_b, \hat{V}_b)$ and $(\hat{P}_c, \hat{V}_c)$ are computed at post-contingency. The pairs (P_{lim},V_{lim}) and ($\hat{P}_{lim}$,$\hat{V}_{lim}$) are the operational limits in pre-and-post contingency, respectively. Note that these limits are defined by the best judgement of the analyst or operator.

The three layers of the index are:

- Single Bus Index (SBI)
- All Buses Index (ABI)
- Global Bus Index (GBI)

The **SBI** is a $\Re^{(2Nb\times 6)}$ matrix where Nb is the number of buses under analysis. SBI provides the distance in pre-and-post contingency for each loading level to the power (P_{lim}) and voltage (V_{lim}) limits of a selected bus or group of buses. SBI is defined in (6) and is divided as follows: columns $1-3$ correspond to the distance for each loading level to the limit with respect to power while columns $4-6$ corresponds to the distance for each loading level to the limit with respect to the voltage. Odd rows refer to pre-contingency data while pair rows refer to post-contingency data. In (6), $P_{i,lim}$ and $V_{i,lim}$ represent the pre-contingency power and voltage limits

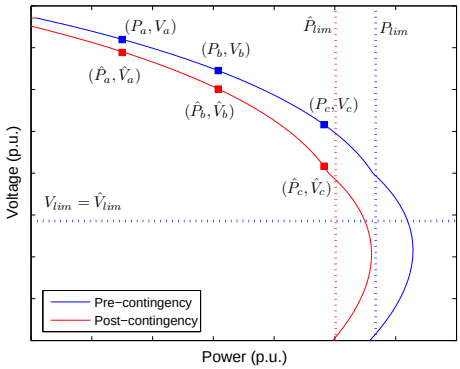

Fig. 2. Pre-and-post contingency PV curves where the power and voltage loading levels are shown: a, b and c for low, acceptable and heavy level, respectively.

at the pth-bus while $\hat{P}_{r,lim}$ and $\hat{V}_{r,lim}$ represent the post-contingency power and voltage limits at the pth-bus, where $p = 1, 2, \cdots, Nb$.

If an element of SBI is negative, then the power or the voltage at some loading level has exceeded the operational limits.

All Bus Index **ABI** is a $\Re^{1\times 6}$ vector that provides the minimum distance among all buses for each loading level to the power and voltage limits, in pre-and-post contingency, as follows:

$$ABI = \left[\Delta\tilde{P}_{a(1,1)}\ \Delta\tilde{P}_{b(1,2)}\ \Delta\tilde{P}_{c(1,3)}\ \Delta\tilde{V}_{a(1,4)}\ \Delta\tilde{V}_{b(1,5)}\ \Delta\tilde{V}_{c(1,6)}\right] \quad (7)$$

$$\Delta\tilde{P}_{(1,j)} = min \left|\begin{matrix} \Delta P_{i,j} \\ \Delta\hat{P}_{r,j} \end{matrix}\right|,\ \Delta\tilde{V}_{(1,k)} = min \left|\begin{matrix} \Delta V_{i,k} \\ \Delta\hat{V}_{r,k} \end{matrix}\right|$$

where $i,\ j,\ r$ and k are defined in (6). The Global Bus Index **GBI** is a 2 element vector that provides the overall minimum distance to the power and voltage limits, respect to all buses. GBI generally indicates if a limit has been violated.

$$GBI = \left[\ \Delta\bar{\mathbb{P}}\ \ \Delta\bar{\mathbb{V}}\ \right] \quad (8)$$

$$\Delta\bar{\mathbb{P}} = min \left|\ \Delta\tilde{P}_{a(1,1)}\ \ \Delta\tilde{P}_{b(1,2)}\ \ \Delta\tilde{P}_{c(1,3)}\ \right|,$$
$$\Delta\bar{\mathbb{V}} = min \left|\ \Delta\tilde{V}_{a(1,4)}\ \ \Delta\tilde{V}_{b(1,5)}\ \ \Delta\tilde{V}_{c(1,6)}\ \right|.$$

Remark. Voltage and power limits considered here are not the theoretical (maximum loadability limits) but the operational limits (an ϵ smaller than the theoretical). Where ϵ is set to the best judgment of the analyst, e.g. $P_{max} = P_{max} - \epsilon P_{max}$.

IV. Computation of the Severity Index using Synthetic Simulations

This section illustrates the use of the proposed index described in Section III and its interpretation. The aim is to calculate the distance from different loading levels to the maximum operational limits in terms of power and voltage.

For this synthetic example a simple system described in Figure 1 was used. Three simulations, each of 30 sec of duration, at different loading levels, were performed. On each simulation the reactance (X) of the line was increased ($2X$) at $t = 15$ sec, to simulate the loss of one line in a transfer

$$SBI=\left[\begin{array}{ccc|ccc} sb_{(1,1)} & sb_{(1,2)} & sb_{(1,3)} & sb_{(1,4)} & sb_{(1,5)} & sb_{(1,6)} \\ sb_{(2,1)} & sb_{(2,2)} & sb_{(2,3)} & sb_{(2,4)} & sb_{(2,5)} & sb_{(2,6)} \\ \hline \vdots & \vdots & \vdots & \vdots & \vdots & \vdots \\ \hline sb_{(n,1)} & sb_{(n,2)} & sb_{(n,3)} & sb_{(n,4)} & sb_{(n,5)} & sb_{(n,6)} \\ sb_{(m,1)} & sb_{(m,2)} & sb_{(m,3)} & sb_{(m,4)} & sb_{(m,5)} & sb_{(m,6)} \end{array}\right] \quad \begin{array}{ll} sb_{(i,j)}=\frac{P_{i,lim}-P_{i,j}}{P_{i,lim}}, & sb_{(i,k)}=\frac{V_{i,k}-V_{i,lim}}{V_{i,lim}}, \\ sb_{(r,j)}=\frac{\hat{P}_{r,lim}-\hat{P}_{r,j}}{\hat{P}_{r,lim}}, & sb_{(r,k)}=\frac{\hat{V}_{r,k}-\hat{V}_{r,lim}}{\hat{V}_{r,lim}}, \\ i=1,3,5,\cdots,n & j=1,2,3 \\ r=2,4,6,\cdots,m & k=4,5,6 \\ m=2Nb & n=m-1. \end{array} \tag{6}$$

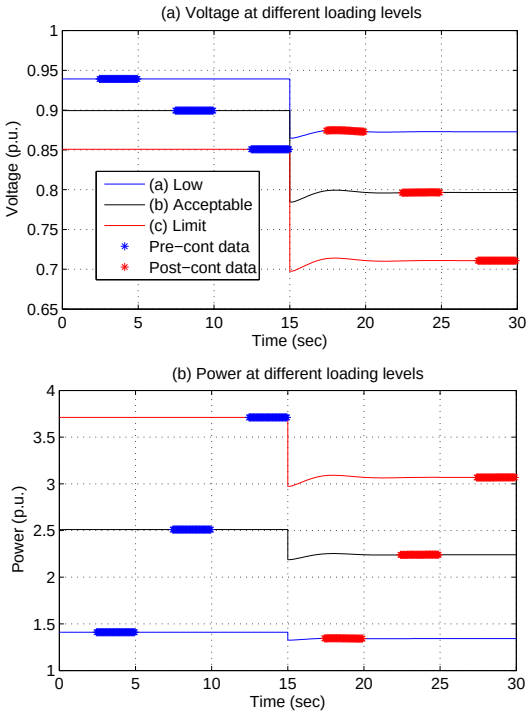

Fig. 3. Set of simulations and data required to calculate the index

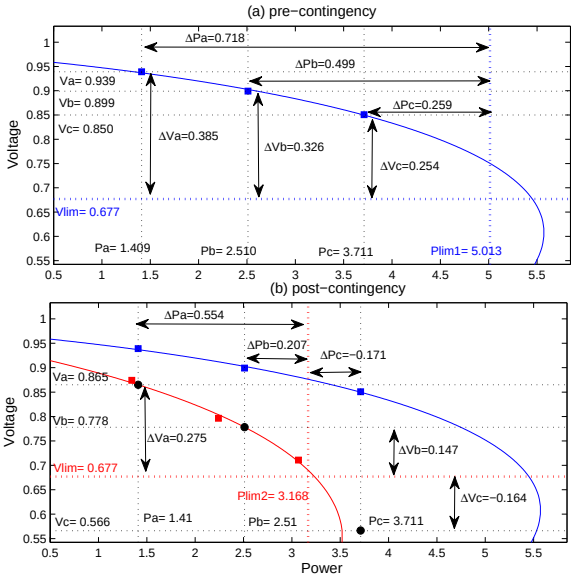

Fig. 4. Estimated PV curves using pre-and-post-fault data, distance to power and voltage limits

corridor of a power system. The set of dynamic simulations required to apply the index are shown in Figure 3 and the estimated PV curves are shown in Figure 4.

Figure 4 (a) and (b) depict the pre-and-post contingency curves in blue and red, respectively. These curves were estimated using the blue and red sections highlighted[2] in Figures 3 (a) and (b), the mean values are shown as squares in Figure 4 and black circles represent the pre-contingency power and voltage levels respect to post-contingency.

In Figure 4 (b), the post-contingency curve (red) is smaller than the pre-contingency curve (blue) because the impedance of the system changed after the disturbance in the network at 15 sec. Note that distances ($\Delta P's$ and $\Delta V's$) in post-contingency are smaller than in pre-contingency and negative in some cases; in post-contingency the power limit decreased and the curve shrinks. Heavy $(\Delta P_c, \Delta V_c)$ loading levels are outside the post-contingency curve; operating the system at this level, the system will be subject to voltage instability following a contingency on the system.

After estimating the equivalent model, the index described in Section III is computed and the results are shown in Table I.

[2]Note that all points from the highlighted section are used in the model identification process (1)-(5).

TABLE I
VOLTAGE STABILITY INDEXES FOR THE SYNTHETIC CASE

				$\Delta\bar{\mathbb{P}}$		$\Delta\bar{\mathbb{V}}$	
GBI				**-0.171**		**-0.164**	
		$\Delta\tilde{P}_a$	$\Delta\tilde{P}_b$	$\Delta\tilde{P}_c$	$\Delta\tilde{V}_a$	$\Delta\tilde{V}_b$	$\Delta\tilde{V}_c$
ABI		0.554	0.207	**-0.171**	0.276	0.148	**-0.164**
		ΔP_a	ΔP_b	ΔP_c	ΔV_a	ΔV_b	ΔV_c
SBI	B_1	0.718	0.499	0.259	0.385	0.326	0.254
	$\hat{B}_1$	0.554	0.207	**-0.171**	0.276	0.148	**-0.164**

GBI is used to interpret the overall results, in this case, both elements of GBI are negative indicating that at least one power and voltage limit was violated. ABI is then used to retrieve more specific information, note that elements $(1,3)$ and $(1,6)$ are negative indicating that there are violations at heavy loading level in both power and voltage $(\Delta\tilde{P}_c, \Delta\tilde{V}_c)$. SBI is finally inspected, observe that elements $(2,3)$ and $(2,6)$ are negative, indicating that post-contingency values for the heavy loading levels $(\Delta\hat{P}_c, \Delta\hat{V}_c)$ are to the right hand side of the power limit and below the voltage limit, as shown in Figure 4 (b), operating the system at this condition will lead to voltage instability.

V. TESTING OF THE INDEX USING THE KTH-NORDIC32 SYSTEM

In this section the proposed index is tested. First the system is described and then different case studies are analyzed.

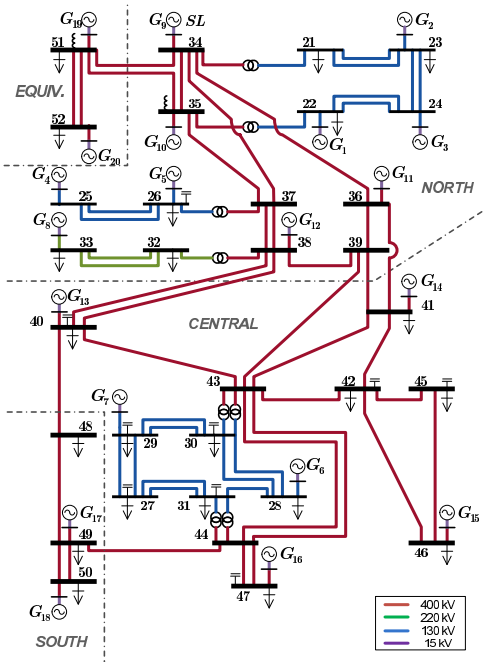

Fig. 5. The KTH-Nordic32 power system.

A. System Description

The KTH-Nordic32 system was constructed from the data proposed in [6], further details are also available in [7]. The system is described in Figure 5 and it has 52 buses, 80 transmission lines and 20 generators, 12 of which are hydro located in the North and equivalent areas, the rest are thermal generators located in the Central and South areas.

The system is heavily loaded with large transfers essentially from North to Central areas. Secure system operation is limited by transient and long-term voltage instability. The contingencies likely to yield voltage instability are: the tripping of a line in the North-Central corridor, forcing the North-Central power to flow over the remaining lines; the outage of a generator located in the Central region, compensated (through speed governors) by the Northern hydro generators, thereby causing an additional power transfer over the North-Central corridor [6].

B. Case study 1: Single Line Trip

In this case study one of the double tie-lines in the Central area, which connects bus 38 with bus 40 was tripped at 10 sec. Three simulations were performed applying the same contingency. Due to space limitations, only the voltage and power at bus 40 are shown on Figure 6. Different loading levels were used for each simulation: an initial load of 88.48 MW (blue lines) was considered, then the load was increased 10% (black lines) and in the last simulation the load was increased 20% with respect to the initial loading level (red lines). Figure 6 illustrates how the voltage at the bus drops as the power increases and, that following the trip of the line, voltage and power suddenly drop from their initial values. Using the pre-and-post contingency data (red and blue sections on Figure 6), the proposed voltage stability index was calculated

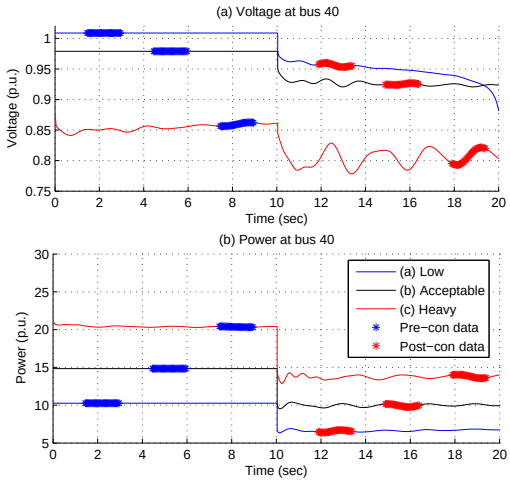

Fig. 6. Set of simulations and data required to calculate the index

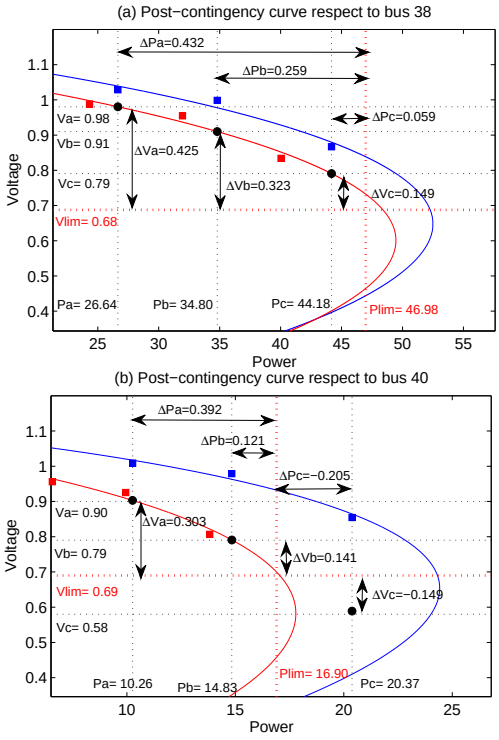

Fig. 7. Estimated PV curves using pre-and-post-fault data, distance to power and voltage limits respect to bus 38 and 40

using signals from buses 38 and 40. The results are displayed on Table II and the pre-and-post contingency curves are shown on Figure 7. In this case study, limits were set to 5% smaller than the theoretical limits ($\epsilon = 0.05$).

B.1 Discussion of results in Case study 1

On Table II both elements of GBI are negative indicating that voltage and power limits were violated at some loading level. Inspection of ABI indicates a violation at heavy loading levels (c), as indicated by the negative numbers of elements $(1, 3)$ and $(1, 6)$. To retrieve more detailed information, SBI is inspected and it is found that both power and voltage limits were violated at heavy loading levels on bus 40, as indicated

TABLE III
VOLTAGE STABILITY INDEXES FOR CASE STUDY 2

		Line Trip C1						Line Trip C2						Line Trip C3						Line Trip C4					
GBI		0.15	0.20					0.16	0.21					**-0.01**	0.10					**-0.04**	0.01				
ABI		0.48	0.30	0.15	0.33	0.27	0.20	0.48	0.30	0.16	0.34	0.28	0.21	0.38	0.16	**-0.01**	0.33	0.24	0.10	0.35	0.13	**-0.04**	0.32	0.21	0.01
SBI	B_{37}	0.52	0.37	0.25	0.46	0.41	0.33	0.52	0.37	0.25	0.46	0.41	0.38	0.52	0.37	0.25	0.46	0.41	0.33	0.52	0.37	0.25	0.46	0.41	0.33
	$\hat{B}_{37}$	0.52	0.37	0.25	0.43	0.37	0.31	0.52	0.38	0.25	0.44	0.38	0.32	0.37	0.17	0.01	0.43	0.32	0.16	0.35	0.16	**-0.01**	0.40	0.38	0.27
	B_{39}	0.48	0.30	0.16	0.35	0.31	0.22	0.48	0.30	0.16	0.35	0.31	0.22	0.48	0.30	0.16	0.35	0.31	0.22	0.48	0.30	0.16	0.35	0.31	0.22
	$\hat{B}_{39}$	0.48	0.30	0.15	0.33	0.27	0.20	0.48	0.30	0.16	0.34	0.28	0.28	0.38	0.16	**-0.01**	0.33	0.24	0.10	0.35	0.13	**-0.04**	0.32	0.21	0.03
	B_{43}	0.52	0.35	0.22	0.44	0.39	0.30	0.52	0.35	0.22	0.44	0.39	0.30	0.52	0.35	0.22	0.44	0.39	0.30	0.52	0.35	0.22	0.44	0.39	0.30
	$\hat{B}_{43}$	0.51	0.35	0.22	0.43	0.36	0.29	0.52	0.35	0.22	0.44	0.37	0.30	0.44	0.24	0.09	0.44	0.34	0.23	0.42	0.22	0.07	0.42	0.33	0.21

TABLE II
VOLTAGE STABILITY INDEXES FOR CASE STUDY 1

				$\Delta\bar{\mathbb{P}}$	$\Delta\bar{\mathbb{V}}$		
GBI				**-0.2058**	**-0.1497**		
		$\Delta\tilde{P}_a$	$\Delta\tilde{P}_b$	$\Delta\tilde{P}_c$	$\Delta\tilde{V}_a$	$\Delta\tilde{V}_b$	$\Delta\tilde{V}_c$
ABI		0.392	0.121	**-0.205**	0.3039	0.141	**-0.149**
		ΔP_a	ΔP_b	ΔP_c	ΔV_a	ΔV_b	ΔV_c
SBI	B_{38}	0.465	0.302	0.114	0.495	0.451	0.260
	$\hat{B}_{38}$	0.432	0.259	0.059	0.425	0.323	0.149
	B_{40}	0.557	0.360	0.121	0.456	0.413	0.233
	$\hat{B}_{40}$	0.392	0.121	**-0.205**	0.303	0.141	**-0.149**

by the negative numbers in elements $(4,3)$ and $(4,6)$ on SBI. Curves on Figure 7 (a) and (b) confirm the results.

C. Case study 2: Multiple Line Trips

In the last case study, 4 contingencies (line outages) were analyzed. Tripping lines between the following buses $51-52$, $35-51$, $35-37$ and $37-38$, labeled as C1, C2, C3 and C4, respectively. For each contingency the proposed VS index was applied respect to three "transit buses"of the KTH-Nordic 32 system (bues 37, 39 and 43), in other words, buses with no load directly connected to it in a transmission corridor or nearby load centers, see [2]. Twelve simulations were performed to produce the results displayed on Table III. Similar to the previous case study, for each contingency, the loading levels were varied in a similar fashion. Twelve PV curves were obtained from these results but they are omitted here due to space limitations. The operational limits used to compute the index were set to 5% smaller than the theoretical limits ($\epsilon = 0.05$) for both powers and voltages.

C.1 Discussion of results in Case study 2

Although neither PV curves nor voltages and power flows of the simulation results are exhibit here due to space limitations, the index results presented on Table III provide all the information required for analysis. The first conclusion from the GBI results is that out of the 4 contingencies analyzed, only C3 and C4 present voltage stability issues in terms of violation of power limits, as indicated by the negative numbers in the elements $(1,1)$ of GBIs C3 and C4, respectively. After analyzing the ABI for all contingencies is possible to conclude that the power violation occurred at heavy conditions and that low and acceptable loading levels are within the limits for all contingencies in all the buses. In this case study, each SBI index is of dimension $\Re^{6\times 6}$ since $Nb = 3$ and $m = 2Nb$. A close look at the SBIs, indicates that only the post-contingency power at bus 39 violates the limits, which means that the post-contingency curve is smaller than the pre-contingency curve for this bus at contingencies C3 and C4. On Table III, SBI results for C1 and C2 predict that post-contingency curves are marginally smaller than pre-contingency curves for all buses, as indicated by the similar values on these SBIs. The index shows that contingencies C1 and C2 do not affect the stability of the system respect to the 3 transit buses.

VI. CONCLUSIONS

In this paper a three-layer index to assess power system voltage stability has been described. The index is calculated using time series from dynamics simulations without any information about the mathematical model of the system. The index is composed of a matrix (SMI), a vector (AMI) and a two element matrix (GMI) to facilitate its interpretation. Time series of the response seen in dynamic simulations of active and reactive power trough transmission lines and voltage at all the buses were utilized as inputs to the index. First, the description of the different layers of the VS index was presented and then an illustrative example using synthetic data was described to facilitate its interpretation .

Nonlinear simulations using the KTH-Nordic32 were performed to validate the proposed index. Future work will focus to the application of this index to time-series obtained from synchronized phasor measurements.

REFERENCES

[1] Y. Sun, P. Wang, L. Cheng, and H. Liu, "Operational reliability assessment of power systems considering condition-dependent failure rate," *Generation, Transmission Distribution, IET*, vol. 4, no. 1, pp. 60–72, 2010.

[2] S. Corsi and G. Taranto, "A real-time voltage instability identification algorithm based on local phasor measurements," *Power Systems, IEEE Transactions on*, vol. 23, no. 3, pp. 1271–1279, Aug 2008.

[3] Y. Kataoka, M. Watanabe, and S. Iwamoto, "A new voltage stability index considering voltage limits," in *Power Systems Conference and Exposition, 2006. PSCE '06. 2006 IEEE PES*, 2006, pp. 1878–1883.

[4] S. Han, B. Lee, S. Kim, and Y. Moon, "Development of voltage stability index using synchro-phasor based data," in *Transmission Distribution Conference Exposition: Asia and Pacific, 2009*, 2009, pp. 1–4.

[5] M. Parniani, J. Chow, L. Vanfretti, B. Bhargava, and A. Salazar, "Voltage stability analysis of a multiple-infeed load center using phasor measurement data," in *Power Systems Conference and Exposition, 2006. PSCE '06. 2006 IEEE PES*, 2006, pp. 1299–1305.

[6] T. Vancustem, "Description, modeling and simulation results of a test system for voltage stability analysis," *Technical Report Version 5, IEEE Working Group on Test Systems for Voltage Stability Analysis*, July 2013.

[7] Y. Chompoobutrgool, W. Li, and L. Vanfretti, "Development and implementation of a nordic grid model for power system small-signal and transient stability studies in a free and open source software," in *Power and Energy Society General Meeting, 2012 IEEE*, 2012, pp. 1–8.